Two-Habit Ice Cloud Model Update and the Scattering Angle Dependence of Retrieved Ice Cloud Optical Thickness

James Coy (Presenting Author), Dongchen Li, Ping Yang

Texas A&M University, Department of Atmospheric Sciences

CERES Science Team Meeting, New York, NY

October 17-19, 2023

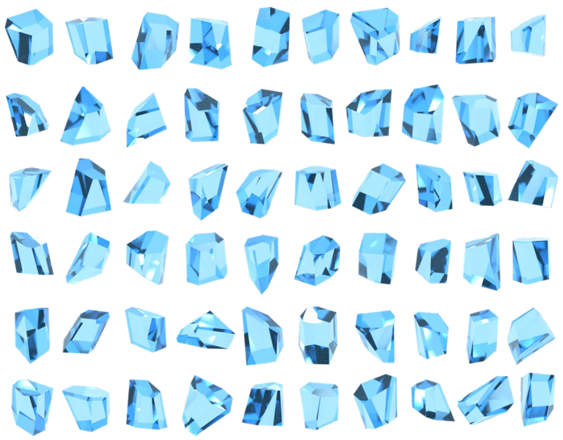

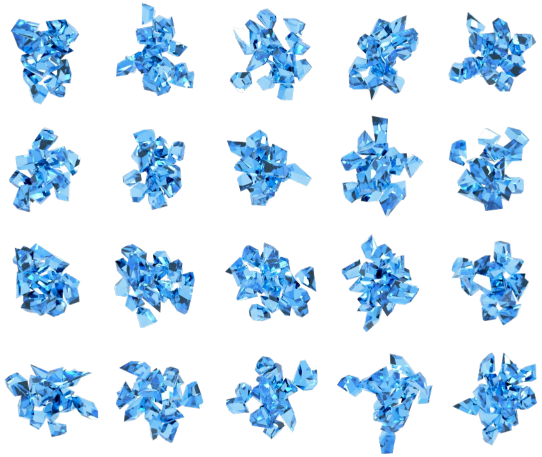

A NASA Consistency Project

- Based on the suggestion that the same ice optical model should be used in a broadband radiation computation and retrieving the cloud description input to the broadband radiation model (Loeb et. al. 2018).

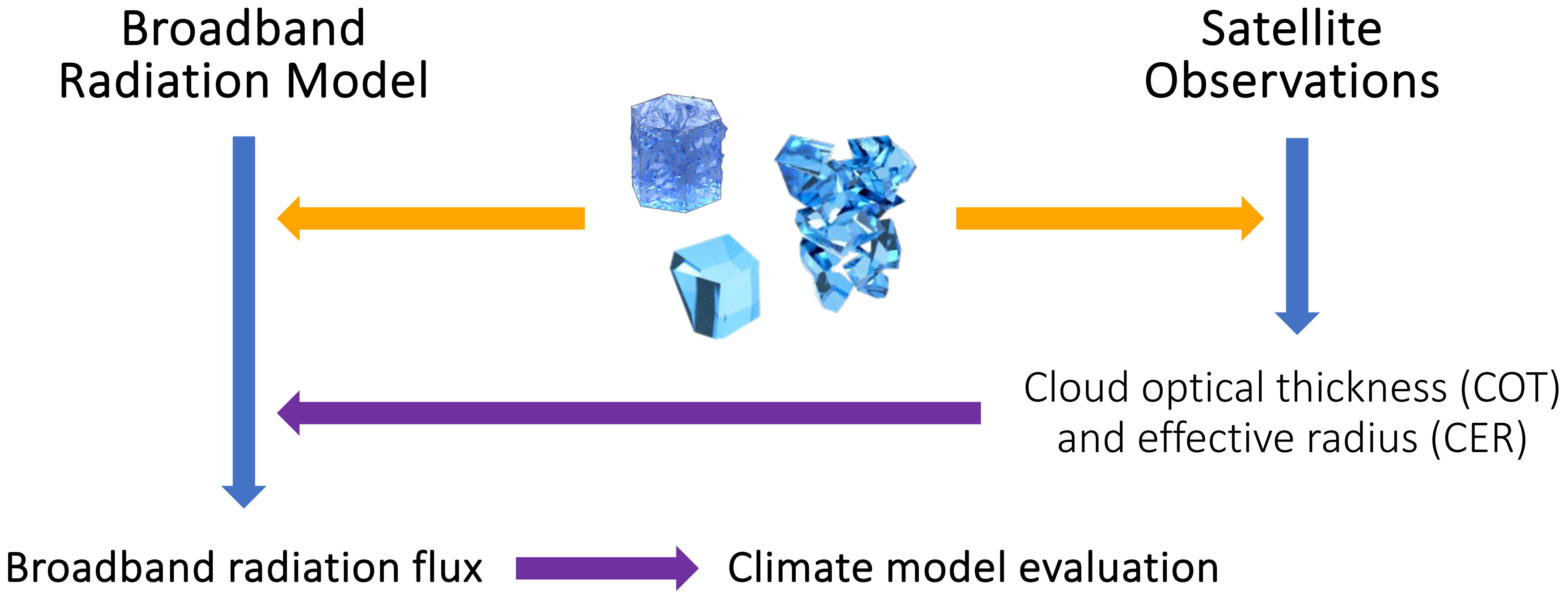

New Broadband Two Habit Model Database (THMv2)

- 60-particle distorted single column and 20-particle distorted aggregate ensembles.
- Builds on the concept of the previously developed THM (Loeb et al. 2018).
- More accurate phase matrix backscattering calculations from Physical Geometric Optics Method (PGOM).
  - Uses ray-tracing technique to analytically obtain electromagnetic near field and subsequently maps it to far field (physical optics).
  - Replaces existing Improved Geometric Optics Method (IGOM) backscattering calculations.

	THM2
Wavelength	470 bins **(0.2 – 200µm)** 3 Lidar bins: **355, 532, 1064nm**
Size (D_{max})	189 bins **(2.206 – 11031.337µm)**

$$f_{single} = \begin{cases} e^{-0.0076(D_{max}-45)}, & D_{max} \geq 45\mu m \\ 1, & D_{max} < 45\mu m \end{cases}$$

$$f_{aggregate} = 1.0 - f_{single}$$

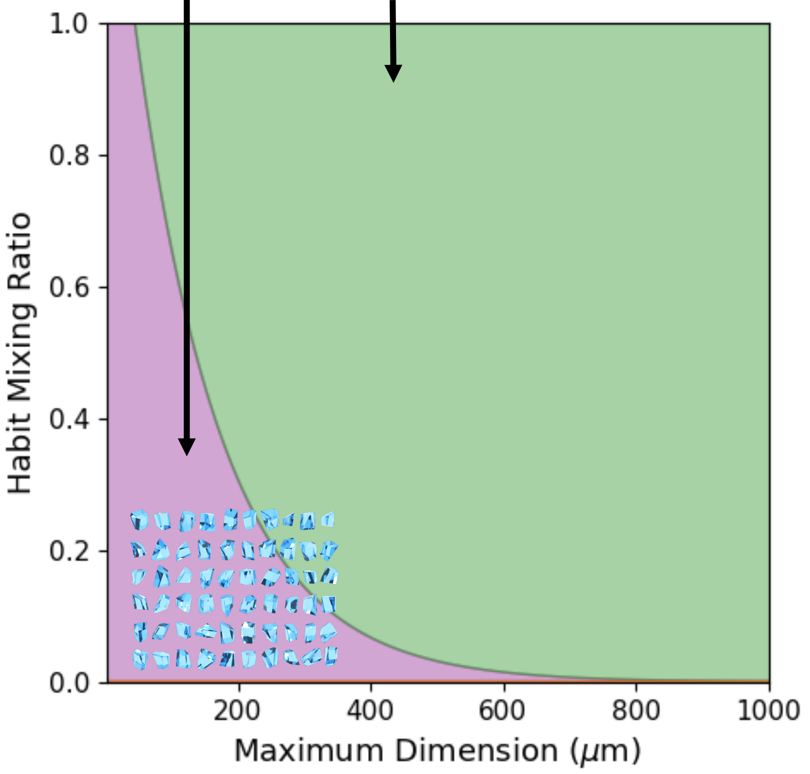

THMv2 Computation Methods

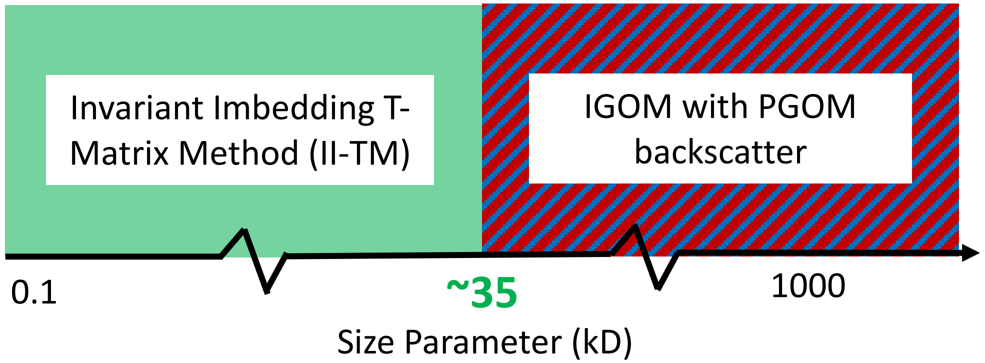

Greater Backscattering!

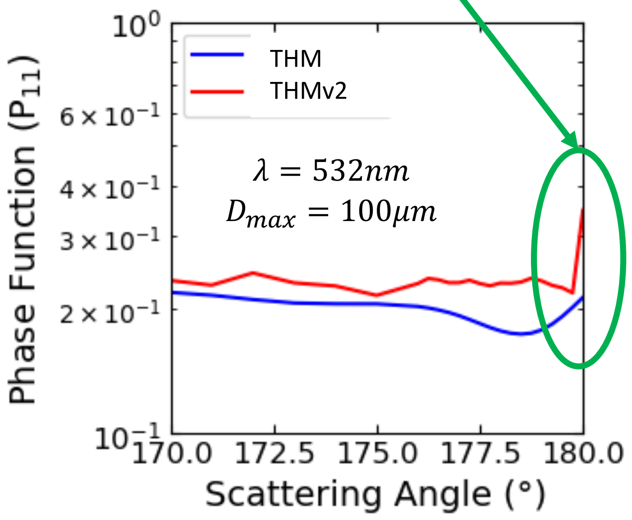

Recap: Progress Utilizing THMv2

- THMv2 radiative parameterization added to Langley Fu-Liou radiative transfer model.
- THMv2 provided improved 532nm backscattering results in lidar ratio and integrated attenuated backscatter consistency with Cloud-Aerosol Lidar with Orthogonal Polarization (CALIOP) observations.
    - Active sensor consistency significantly improved.

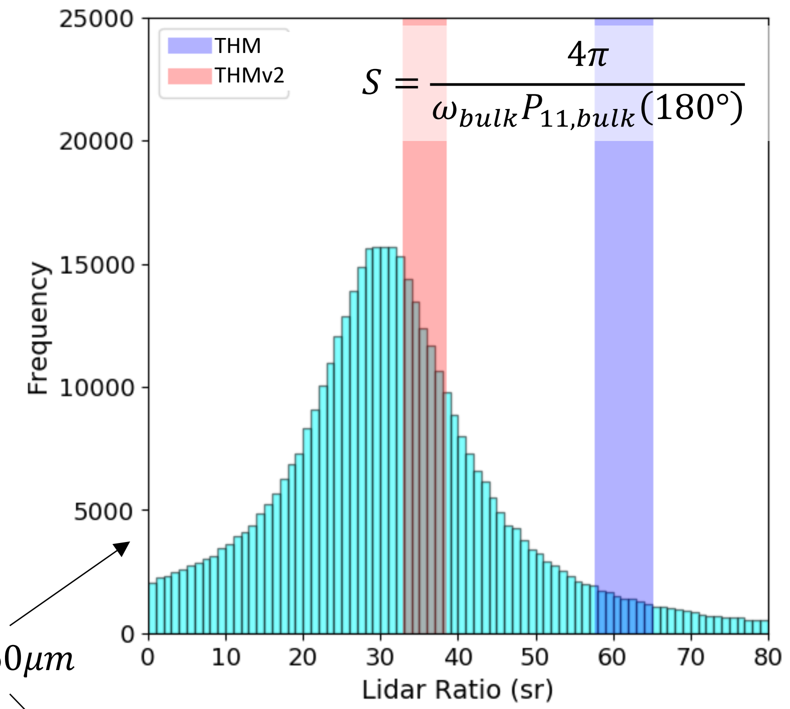

$n = 491759$

$20\mu m \leq R_{eff} \leq 60\mu m$

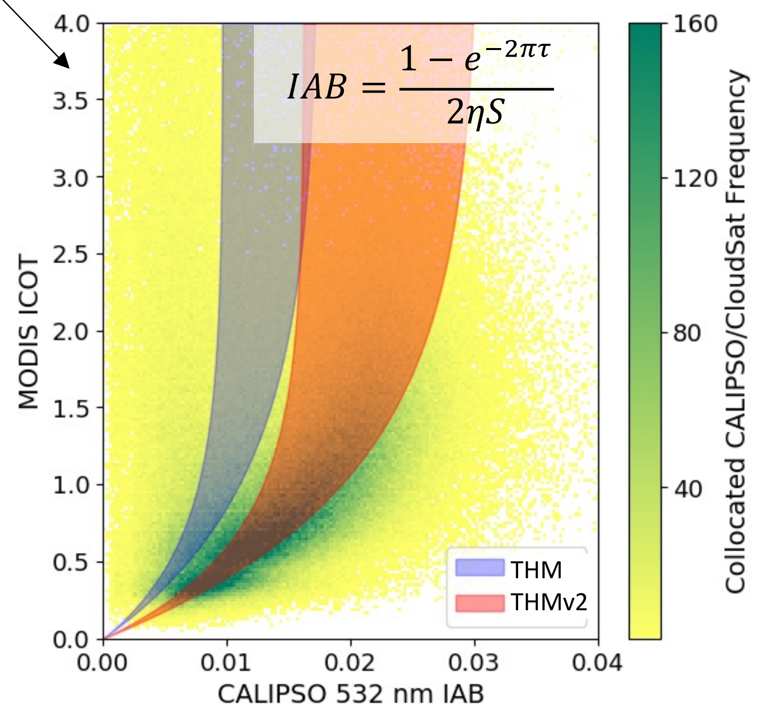

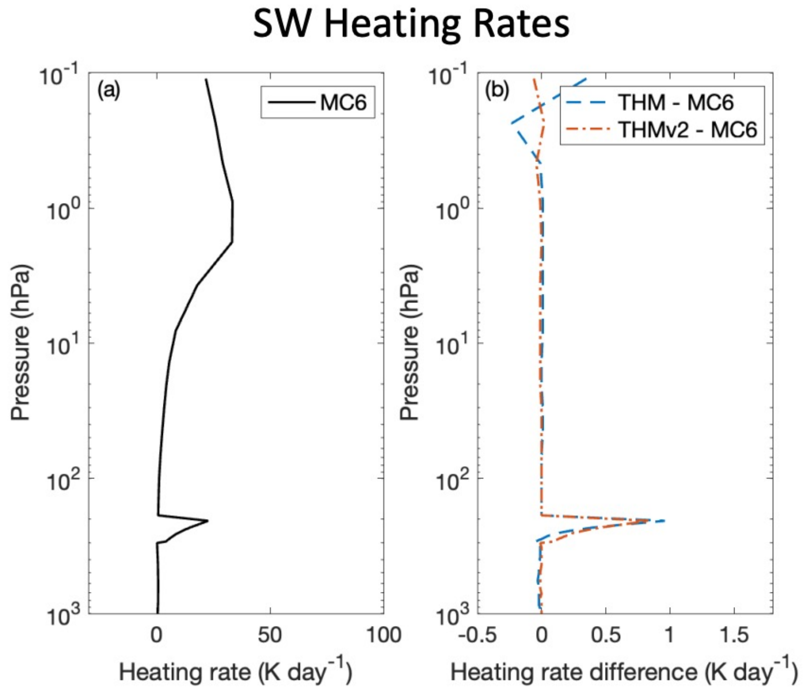

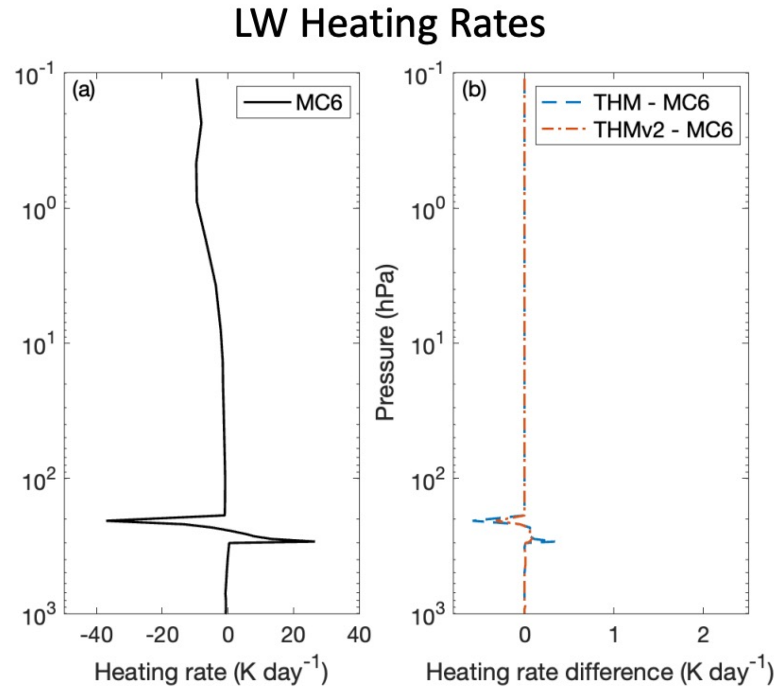

Scattering Angle Dependence of the Spectral Consistency of Ice COT Retrievals based on Geostationary Observations

- Utilize the Advanced Baseline Imager (ABI) on board the Geostationary Operational Environmental Satellites – 16/17 (GEOS-16/17).
  - o 16-band radiometer covering visible (VIS) to infrared (IR) portions of the spectrum.
- **Shortwave and longwave reflectance data used to retrieve COR and CER from look-up tables (LUT) of simulated ice cloud reflectances that use THMv2.**
- Mitigation of retrieval failures achieved by filtering out low quality pixels:
  - o High sunglint effect ($< 30°$).
  - o High multilayer cloud effect (reflectance ratio $k < 2.5$).
    - ▪ Reflectance band 2 ($R_{band,2}: 0.64\mu m$) increases with greater contribution from lower layer clouds which increases k.

$$k = \frac{R_{band,2} - R_{sfc}}{R_{band,4}}$$

GOES-17

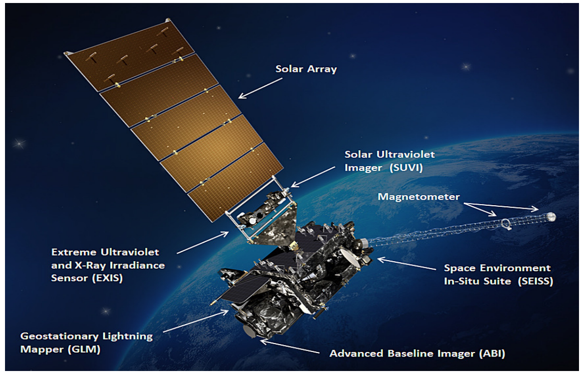

GOES-17 ABI Pixel Data Acceptance Criteria	
Variable name	Threshold for acceptance
Cloud top phase	Ice
Solar Zenith Angle (SZA)	< 60°
Latitude	$81.3282° S - 81.3282° N$
Longitude	$141.9° E - 55.9° W$
Viewing Zenith Angle (VZA)	< 80°
Surface type mask	Ocean
Day/Night flag	Day
Sunglint angle	> 30°
k	< 2.5

Nakajima-King VIS/NIR Retrieval Method

- In forward model of Visible/Near-Infrared (NIR) retrieval system, adding-doubling radiative transfer model (RTM) used to construct LUT.
  - LUT contains combinations of COT, CER, and corresponding reflectance.

$$y = F(x, b) + e$$

- Where F is the forward model and e is the measurement model error.

$$x = \begin{pmatrix} COT \\ CER \end{pmatrix}, \quad y = \begin{pmatrix} R_{band\ 2} \\ R_{band\ 6} \end{pmatrix}, \quad b = \begin{pmatrix} \mu \\ \mu_0 \\ \phi \\ \alpha_{sfc} \end{pmatrix}$$

- Where x, y, and b are the state, measurement, and model parameter vectors, respectively.

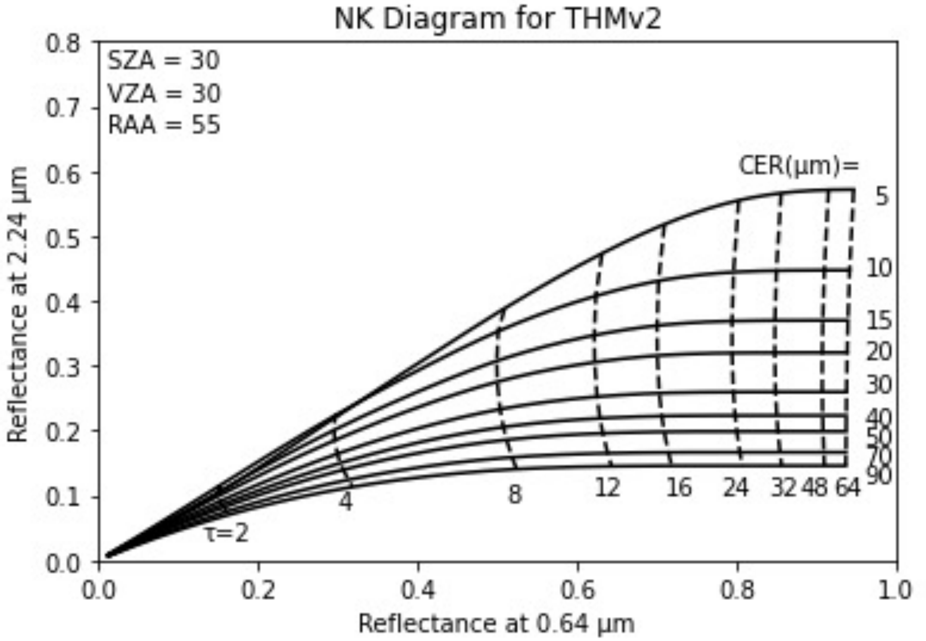

VIS/NIR retrieval inputs	Data source
Band 2 (0.64 μm)	GOES-17
Band 6 (2.24 μm)	GOES–17

Split-Window IR Retrieval Method

- Single-layer RTM based on two-stream approximation used in forward model of the thermal IR (TIR) retrieval system.

$$y = F(x, b) + e$$

$$x = \begin{pmatrix} COT \\ CER \\ CTT \end{pmatrix}, \quad y = \begin{pmatrix} BT_{band\ 11} \\ BT_{band\ 13} \\ BT_{band\ 14} \\ BT_{band\ 15} \end{pmatrix}, \quad b = \begin{pmatrix} \mu \\ w \\ \varepsilon_{sfc} \\ P_{atm} \\ SST \end{pmatrix}$$

Cost function:

$$J(\mathbf{x}) = (\mathbf{x} - \mathbf{x}_a)^{\mathrm{T}} \mathbf{S}_a^{-1} (\mathbf{x} - \mathbf{x}_a) + [\mathbf{y} - \mathbf{F}(\mathbf{x}, \mathbf{b})]^{\mathrm{T}} \mathbf{S}_y^{-1} [\mathbf{y} - \mathbf{F}(\mathbf{x}, \mathbf{b})]$$

- Where $\mathbf{x}_a$ is an a priori vector, $\mathbf{S_a}$ is the error covariance matrix of the a priori, and $\mathbf{S_y}$ is the covariance matrix of the measurement-model error.

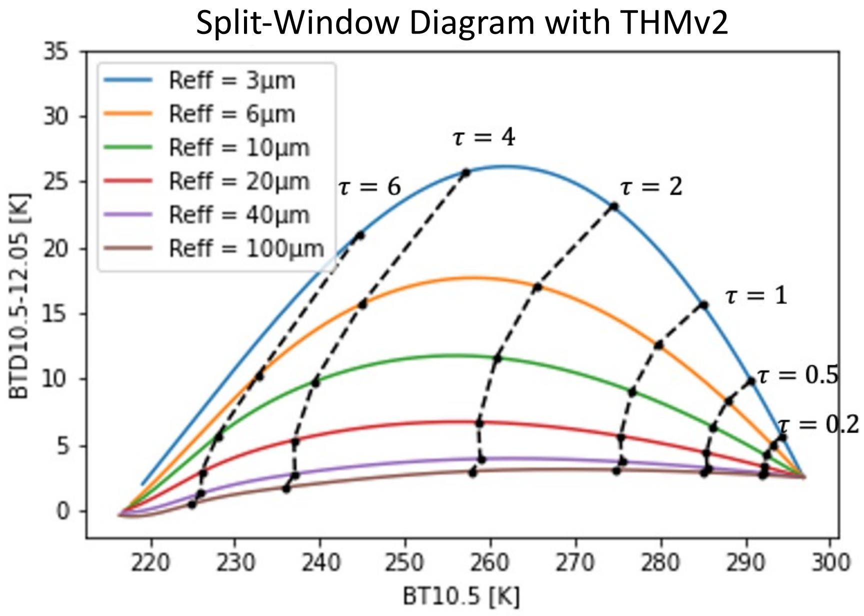

IR retrieval inputs	Data source
$Band_{11,13,14,15}$ (8.4 μm, 10.3 μm, 11.2 μm, 12.3 μm)	GOES-17
Cloud Top Temp. (CTT)	GOES-17
P_{atm}, w	MERRA-2
Sea Surface Temp. (SST)	JPL PO.DAAC

Spectral Consistency of COT from GOES-17 Observations

- COT 2-dimensional frequency distribution created using 1 hour GOES-17 observations from 20:00 – 20:50 UTC on Sept. 23, 2019.

- THMv2 achieves best spectral consistency.

- Are there any factors that can introduce biases/uncertainties from VIS-NIR and TIR retrieval methods?
  - Would the THM spectral consistency be negatively impacted?

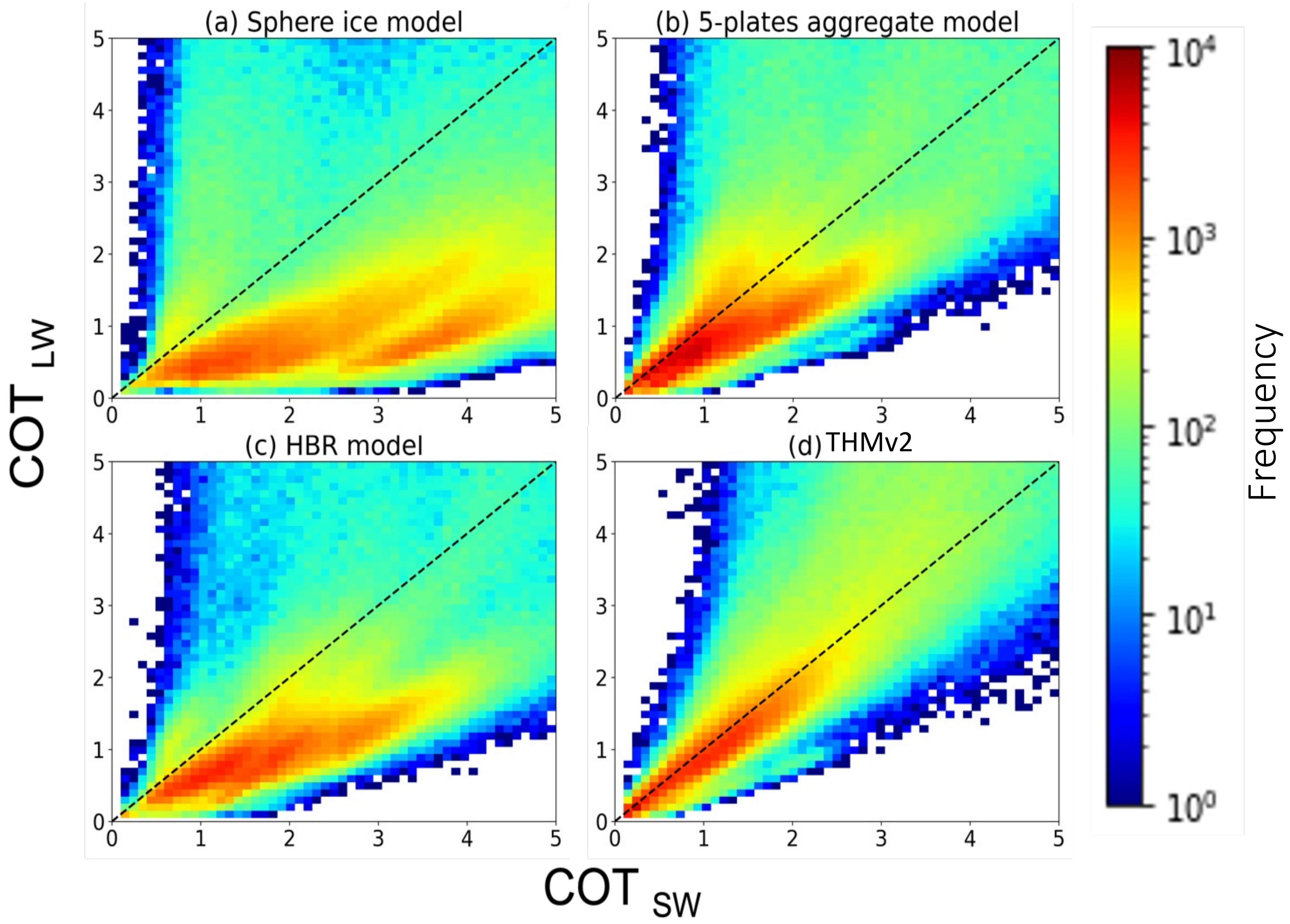

Angular Dependence of the COT Ratio (COT_{SW} / COT_{LW})

- Ice particle models with consistent optical properties with particles in natural clouds should result in 1:1 COT ratio.
- Fig. (a) shows median value COT ratio significant angular dependence.
  - Optically thin clouds (COT<1)
  - Very cold CTT (< 210 K)
- Angular dependence of COT will likely result in biased retrievals even though THMv2 is used.
  - **What is the cause?**

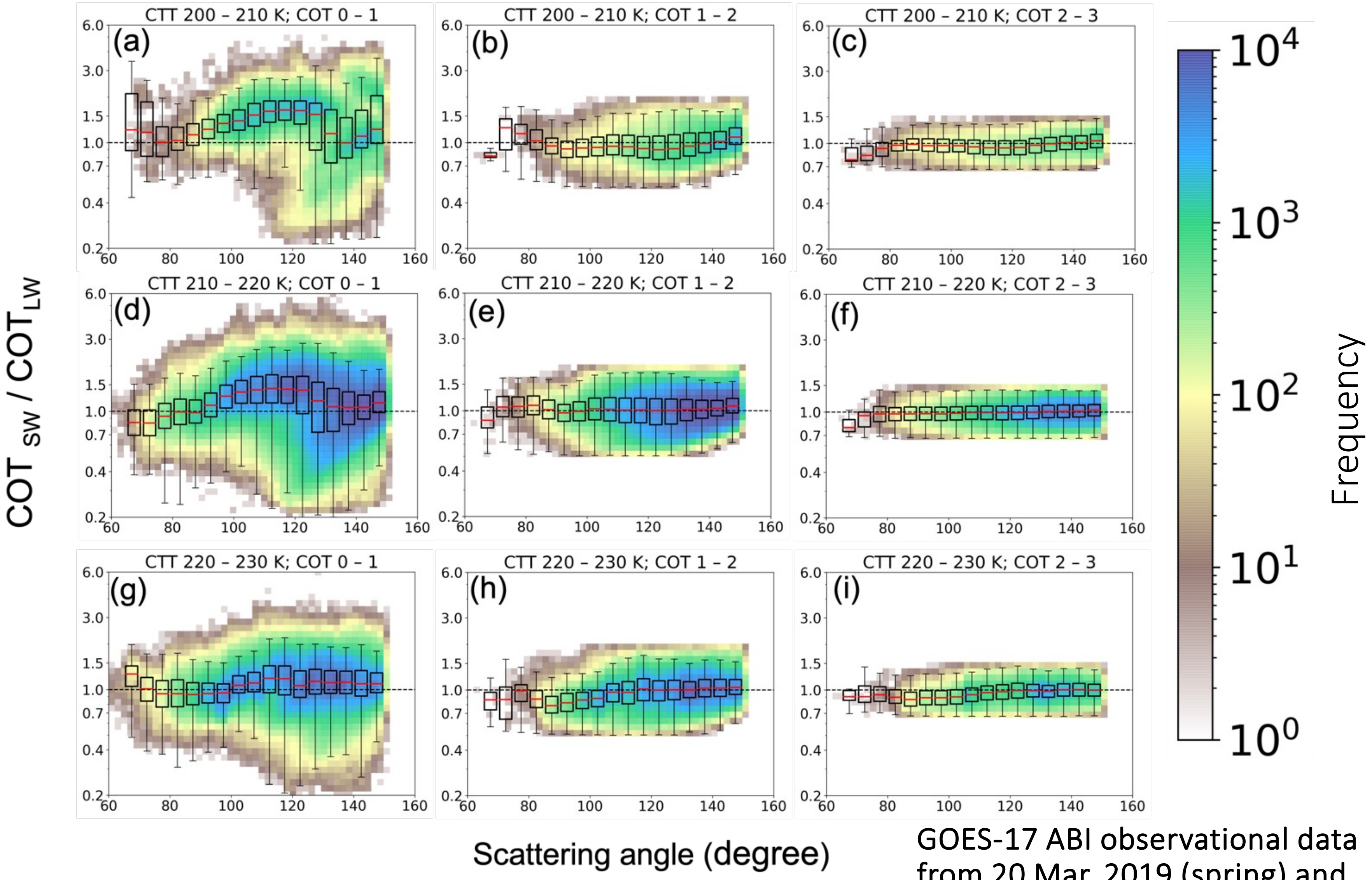

GOES-17 ABI observational data from 20 Mar. 2019 (spring) and 23 Sept. 2019 (fall)

Narrowing Down COT Ratio Angular Dependence: SZA

- COT 0 – 1, SZA $0° - 20°$ (a)
  - COT ratio remains < 1 but increases with increasing scattering angle.
- COT 0 – 1, SZA $20° - 60°$ (d)
  - Majority of COT ratio > 1 and shows irregular variation with scattering angle.
- COT > 1:
  - Uncertainties and variation of COT ratio decrease as COT increases within same CTT range.

$200K \leq CTT \leq 210K$

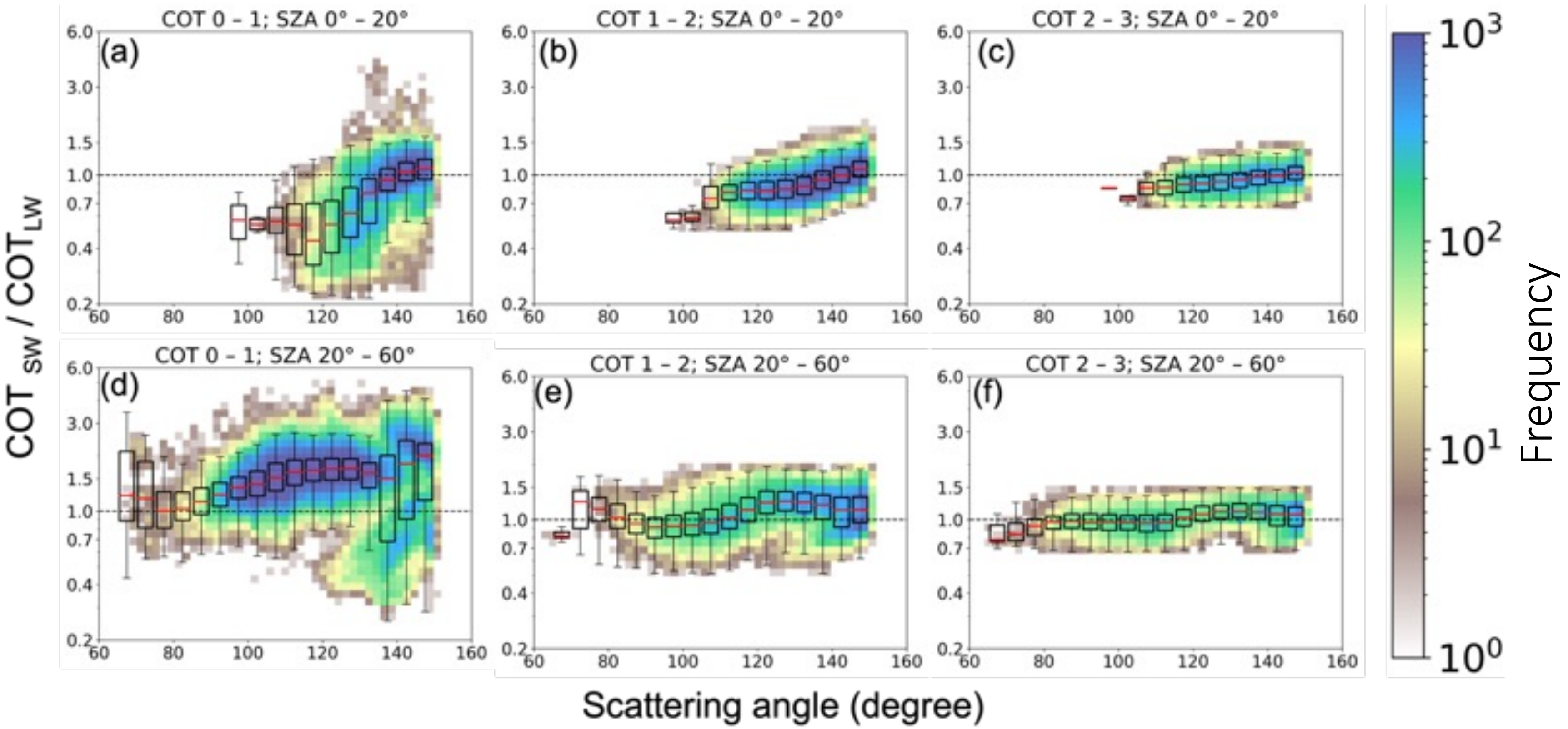

Potential Impact from Mixed-Phase Clouds

- Current cloud-top phase classification algorithm employed by GEOS-17 relies mainly on empirical thresholds at multiple infrared wavelengths.
  - Could introduce potential biases on the discrimination of cloud phase (Hu et al. 2021).

- Thermal based cloud top phase retrievals are sensitive to errors, particularly in detecting optically thin and broken clouds (Wolters et al. 2008).

- Due to misidentification of cloud phase and inhomogeneity of clouds within pixels, the optical property retrievals of thin ice clouds could be potentially affected by the liquid or mixed-phase clouds.

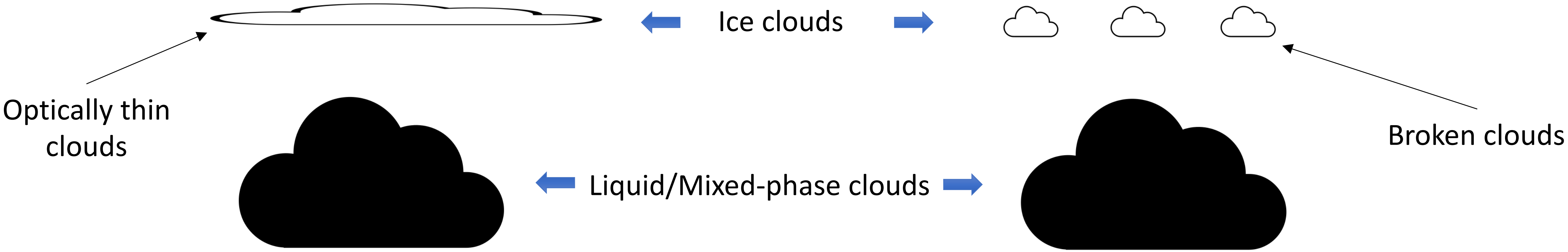

Mixed-Phase Bulk Optical Property Calculation

- **Mixed-phase cloud**: mixture of the volumes of ice and liquid clouds within the vertical column of a pixel.
- The **effective radius ($\boldsymbol{r_{eff}}$)** of ice and liquid particles is defined as: $r_{eff} = \frac{3}{4}\frac{\langle V\rangle}{\langle A\rangle}$
  - Where $\langle V\rangle$ is the bulk particle volume, $\langle A\rangle$ is the bulk particle projected area.
- The **liquid volume fraction ($\boldsymbol{f^l}$)** is defined as: $f^l = \frac{\langle V^l\rangle}{\langle V^l\rangle+\langle V^i\rangle}$
  - The superscripts "l", "i", and "m" represent liquid, ice, and mixed-phase, respectively.

Projected area weighted fraction

$$f_A^l = \frac{\frac{f^l}{{r_{eff}}^l}}{\frac{f^l}{{r_{eff}}^l}+\frac{1-f^l}{{r_{eff}}^i}},$$

Extinction cross section weighted fraction

$$f_{ext}^l = \frac{\frac{\langle Q_{ext}^l\rangle f^l}{{r_{eff}}^l}}{\frac{\langle Q_{ext}^l\rangle f^l}{{r_{eff}}^l}+\frac{\langle Q_{ext}^i\rangle(1-f^l)}{{r_{eff}}^i}},$$

Scattering cross section weighted fraction

$$f_{sca}^l = \frac{\frac{\langle Q_{sca}^l\rangle f^l}{{r_{eff}}^l}}{\frac{\langle Q_{sca}^l\rangle f^l}{{r_{eff}}^l}+\frac{\langle Q_{sca}^i\rangle(1-f^l)}{{r_{eff}}^i}},$$

$$\langle Q_{ext}^m\rangle = \langle Q_{ext}^l\rangle f_A^l + \langle Q_{ext}^i\rangle(1-f_A^l),$$
$$\langle \omega^m\rangle = \langle \omega^l\rangle f_{ext}^l + \langle \omega^i\rangle(1-f_{ext}^l),$$
$$\langle g^m\rangle = \langle g^l\rangle f_{sca}^l + \langle g^i\rangle(1-f_{sca}^l),$$
$$\langle P_{11}^m\rangle = \langle P_{11}^l\rangle f_{sca}^l + \langle P_{11}^i\rangle(1-f_{sca}^l).$$

Where $\langle Q_{ext}\rangle$ is bulk extinction efficiency, $\langle Q_{sca}\rangle$ is bulk scattering efficiency, $\langle \omega\rangle$ is bulk single scattering albedo, $\langle g\rangle$ is bulk asymmetry factor, and $\langle P_{11}\rangle$ is bulk phase function

Nakajima-King (a-c) and Split-Window (d-f) diagrams for THMv2, Mixed-Phase ($f = 0.5$), and Liquid Model.

- Nakajima-King:
  - SZA = $30°$
  - VZA = $60°$
  - RAA = $20°$
- Split-Window:
  - VZA = $60°$
  - CTT = 250 K
  - SST = 297 K
  - 17.82 mm precipitable water
  - Surface emissivity = 0.99

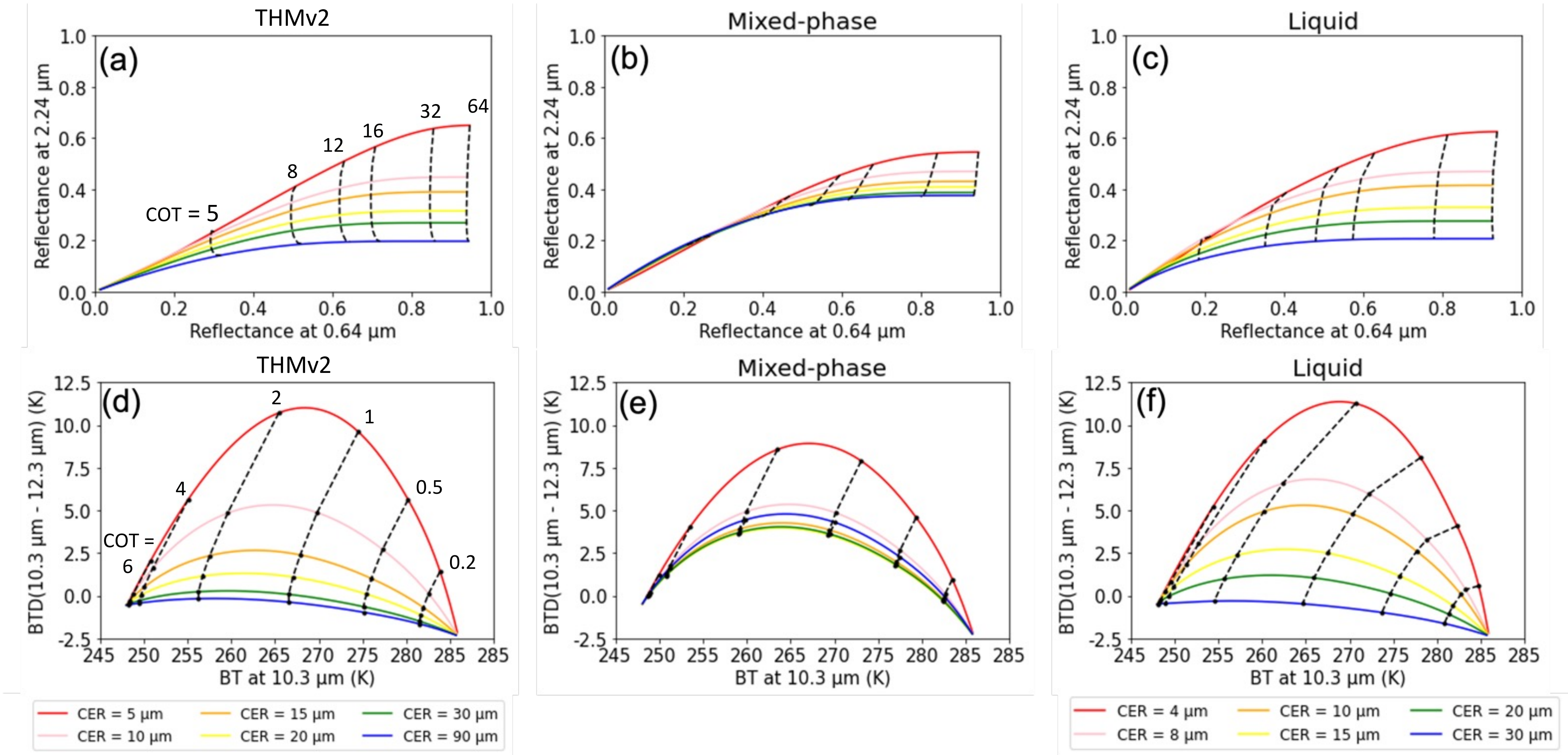

- Fig. b shows severe nonorthogonal correlation between COT and CER when COT < 8.
  - Indicates the challenge to obtaining the optimal solutions using VIS-NIR retrieval method based on the mixed-phase model.
- Although optical properties of liquid droplets have nonnegligible impact on the CER of mixed-phase cloud at TIR channels, COT of mixed-phase cloud is less affected by liquid droplets compared to VIS and NIR channels.

Phase Function Ratio Comparisons Between Ice and Mixed Phase Clouds

- $\langle P_{11} \rangle$ of THMv2 (blue) almost independent of scattering angle.
- $\langle P_{11} \rangle$ of liquid droplets show variations in near backscattering region.
  - Variation of $\langle P_{11} \rangle$ ratio increases with increasing liquid volume fraction (f).
  - Peak observed at the $140°$ scattering angle known as the "rainbow peak".
- **Angular dependence of $\langle \boldsymbol{P_{11}} \rangle$ ratio could contribute to variation of COT ratio with respect to scattering angle.**

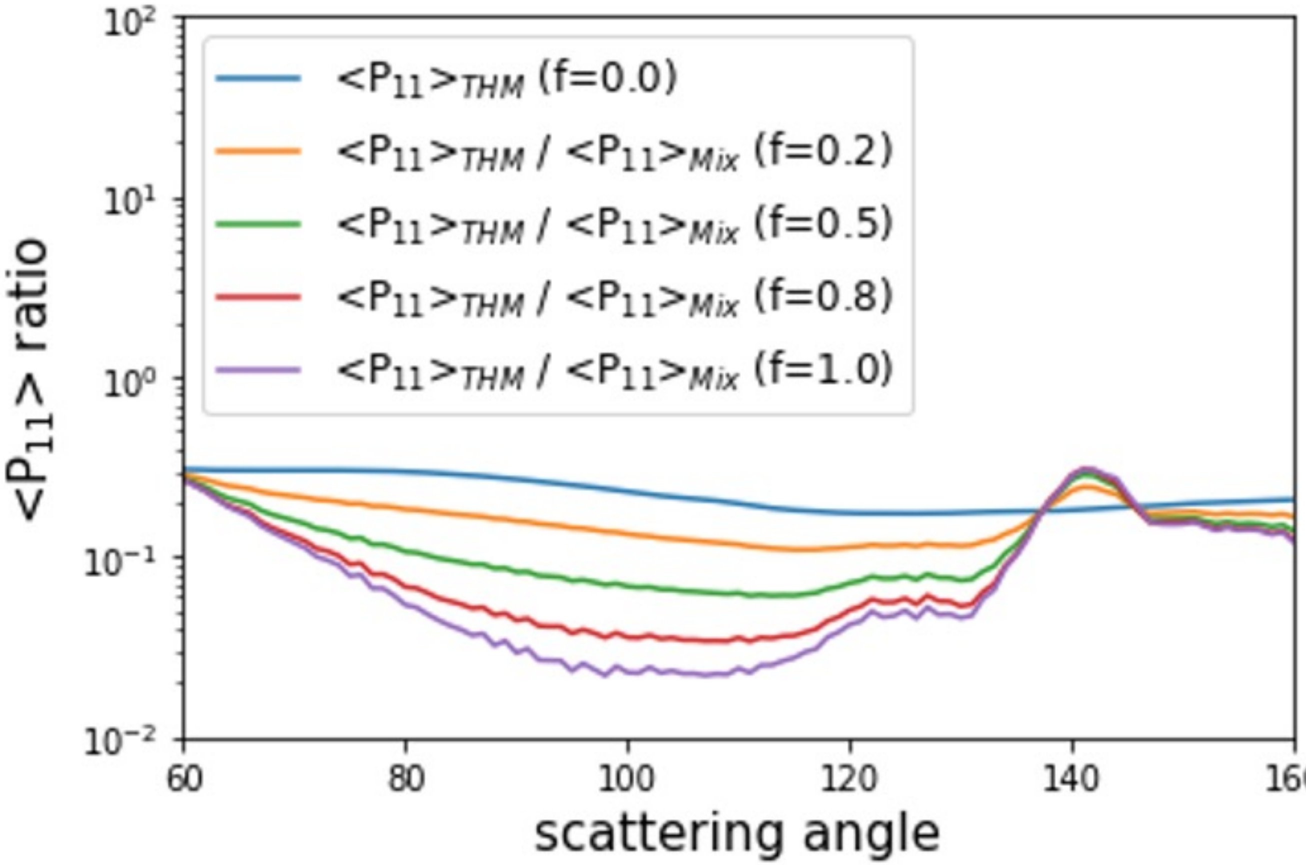

$\langle P_{11} \rangle$ of THMv2 and the $\langle P_{11} \rangle$ ratio of THMv2 and mixed-phase model with various liquid volume fraction in scattering angle 60 to 160 degree at 0.64 μm wavelength. The CER of THMv2 is 33.01 μm. The CER of mixed-phase model (CER_{mix}) is obtained by combining the CER of 33.01 μm for ice particles and the CER of 10 μm for liquid droplets.

Flow Chart of Simulation Process for Evaluating Impact of Mixed-Phase Cloud on the Spectral Consistency of COT

- COT retrieved from LW method used in both SW and LW retrieval systems.
  - Less mixed-phase cloud impact on LW method retrieval results.
- Simulated COT results retrieved using THMv2 in SW and LW methods.

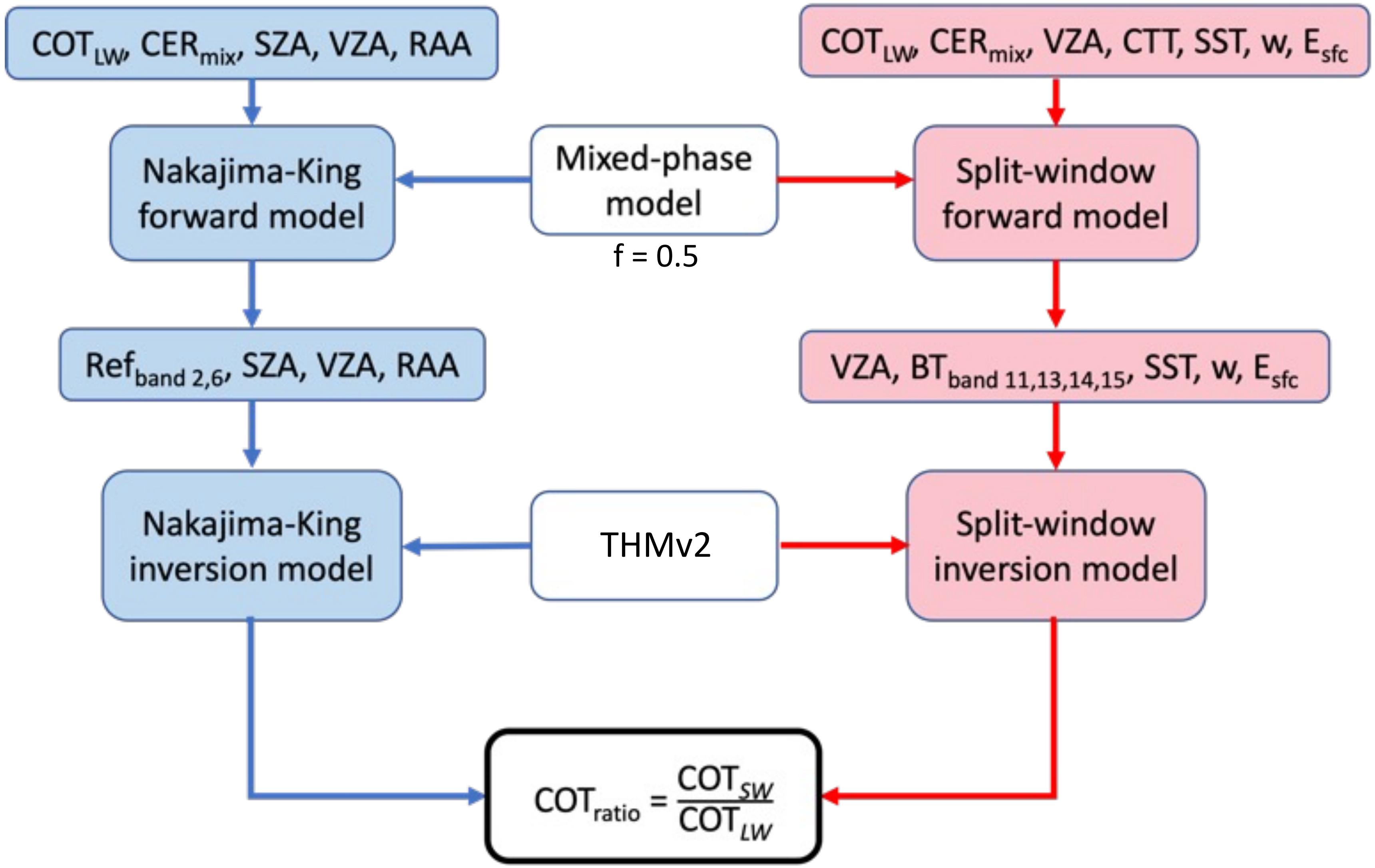

Mixed-Phase Cloud Impact on the Spectral Consistency of COT Results

- When ice cloud is optically thin (COT < 1), single-scattering properties play significant role in overall radiative transfer (a).
  - Variation of simulated COT ratio reflects changes in $\langle P_{11} \rangle$ with respect to scattering angle.
- Contribution of multiple scattering to solar reflectance from clouds increases as COT increases.
  - $\langle g \rangle$ has more pronounced impact on radiative transfer than $\langle P_{11} \rangle$.
  - $\langle g \rangle$ of mixed-phase cloud larger than ice cloud, retrieved COT from mixed-phase cloud using VIS-NIR method based on THMv2 can be underestimated.

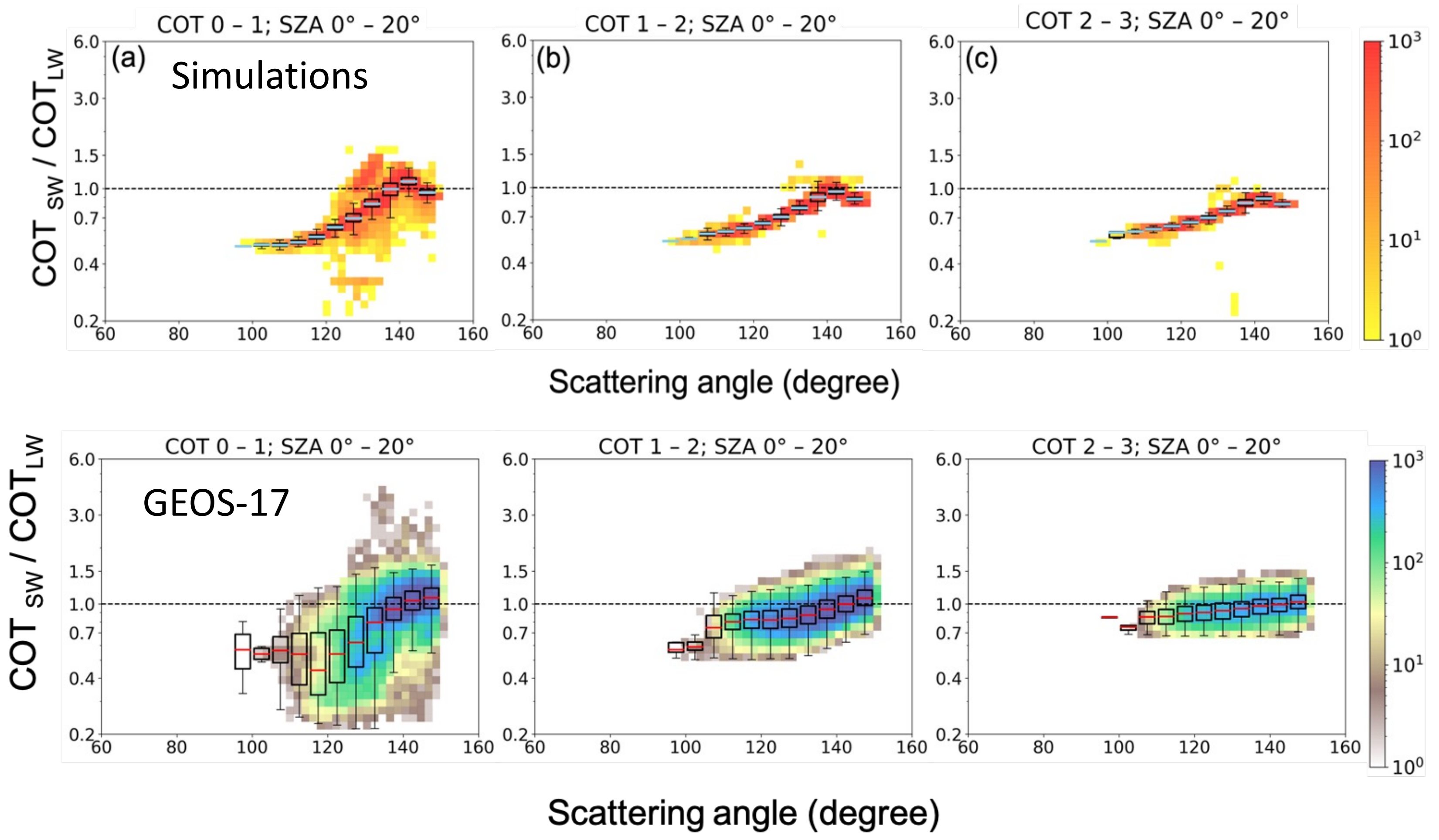

Flow Chart of Simulation Process for Evaluating Impact of CTT and SST on the Spectral Consistency of COT

- Mixed-phase cloud effect did not explain positive biases in COT ratio when SZA is large.
  - Answer could be in longwave retrievals.
- CTT and SST important variables in LW retrieval process.
  - GEOS-17 exhibits slight overestimation of ice cloud CTT compared with CALIPSO (Lima et al. 2019).
  - SST retrieved from TIR restricted to clear-sky leading to overestimation.
- CTT and SST negative biases implemented into LW retrieval method to counteract overestimations.

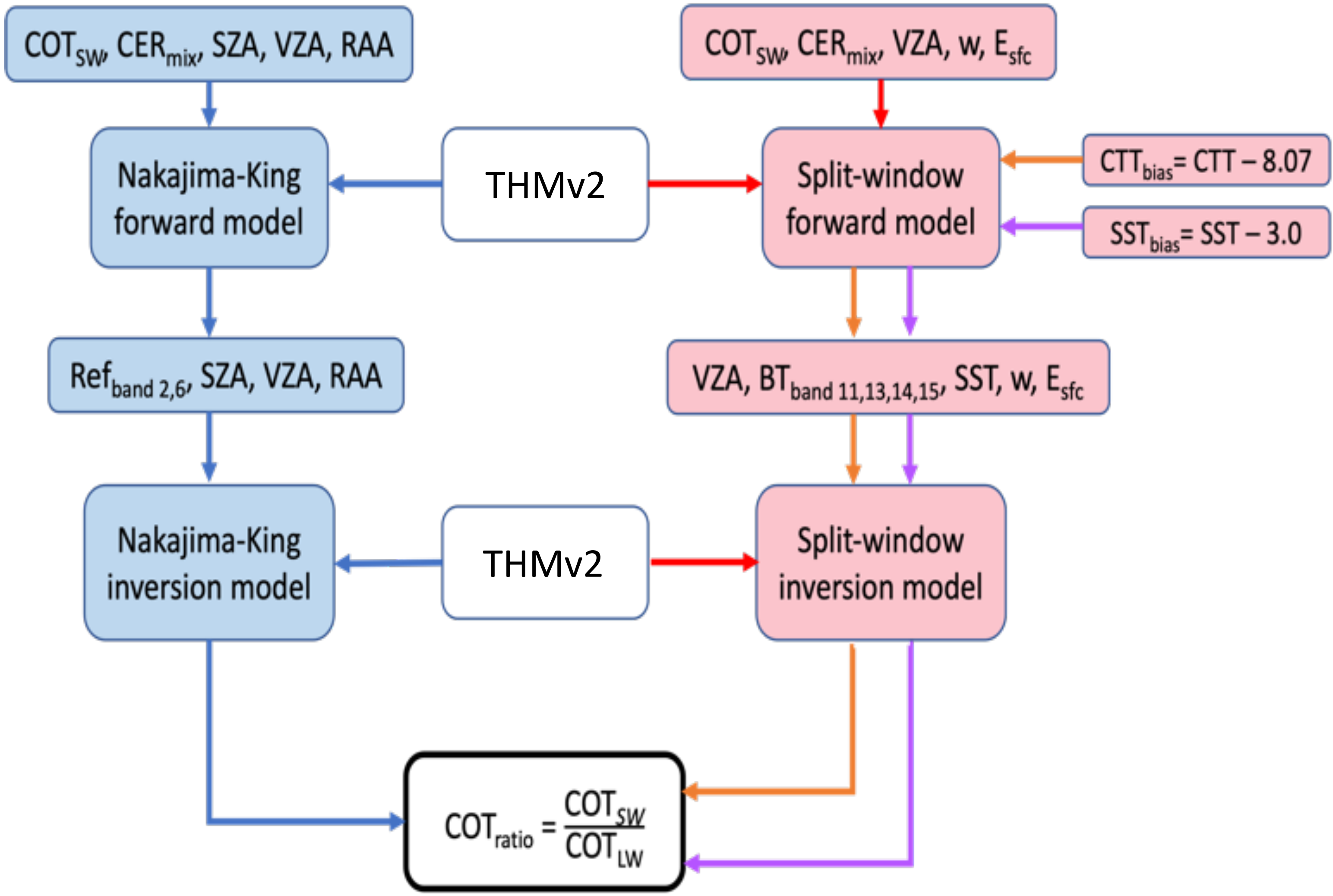

Simulation Results of COT Ratio With Consistent Ice Particle Model on Biased CTT (a) and SST (b)

- Less variation of COT ratio across scattering angle range, resulting in small negative biases.
- Negative biases in CTT and SST lead to underestimation of brightness temperature.
  - Results in higher COT retrievals from LW method, inducing negative biases in simulated COT ratio results.
- However, COT ratio > 1 (positive bias) from observations when SZA > $20°$.
  - Potential biases in VIS-NIR method could be the cause.
  - Cloud 3D effect becomes prominent as VZA and SZA increases for heterogeneous clouds (Loeb et al. 1997).

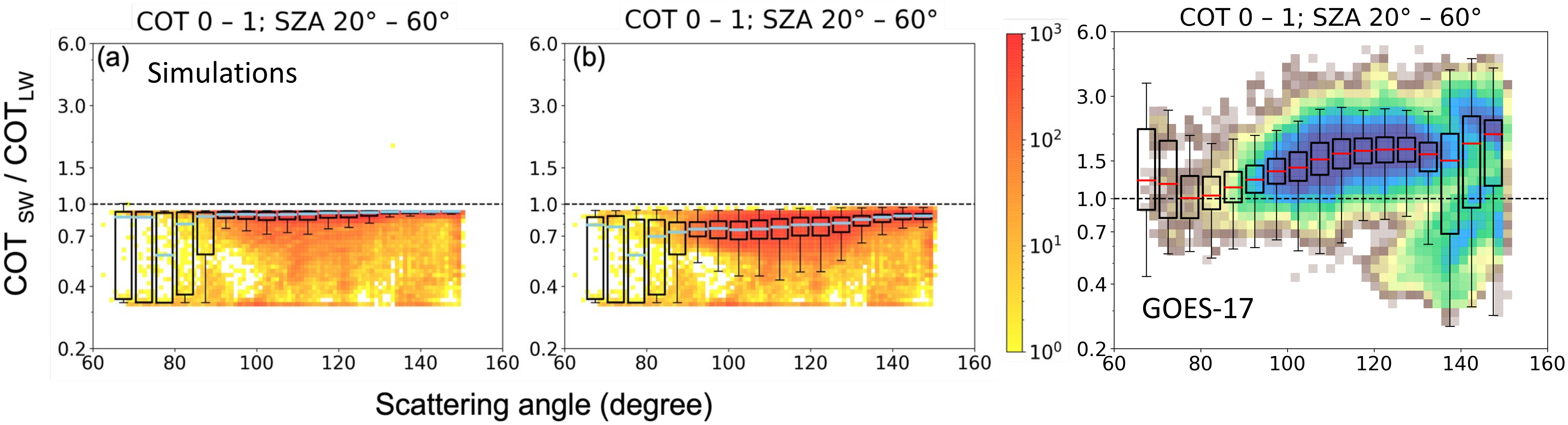

Summary and Future Work

- THMv2 achieves optimal COT spectral consistency from GOES-17 observations.
  - An instance of active-passive consistency due to THMv2 having significantly improved lidar retrieval results due to improved backscattering.
- Angular dependence of COT ratio discovered in observations for optically thin clouds (COT < 1) despite optimal THMv2 spectral consistency.
  - SZA $< 20°$, influence of mixed-phase clouds become prominent in generating negative angular dependence bias.
  - SZA $> 20°$, cloud 3D effect could be dominant factor that causes positive angular dependence bias.
- Angular dependence of COT ratio could help identify mixed-phase clouds and their impact on spectral consistency of COT.

- Plans to compare broadband flux RTM calculations utilizing THMv1, THMv2, and other conventional ice particle single-scattering databases against CERES observations.
  - Further confirm active-passive consistency of THMv2 database.
- An updated MODIS Collection 6 single-scattering database inspired by THMv2 recently developed.
  - 20-particle ensemble of distorted 8-column aggregates with improved backscattering from PGOM

Upcoming Manuscripts

Li, D., Saito, M., Yang, P., Loeb, N. G., Smith Jr., W. L., and Minnis, P. (2023). On the scattering-angle dependence of the spectral consistency of ice cloud optical thickness retrievals based on geostationary satellite observations. IEEE Transactions on Geosciences and Remote Sensing. (Forthcoming - submitted)

lidc@tamu.edu (Dongchen Li)

Coy, J., Saito, M., Yang, P., Liu, X., and Hu, Y. (2023). A robust ice cloud optical property model for lidar-based remote sensing applications. *IEEE Geoscience and Remote Sensing Letters*. (Forthcoming – submitted)

jcoy93@tamu.edu (James Coy)

References

Hu, J., Rosenfeld, D., Zhu, Y., et al. (2021). Multi-channel Imager Algorithm (MIA): A novel cloud-top phase classification algorithm. *Atmospheric Research*. **261**(15), 105767.

Lima, C. B., Prijith, S. S., Sesha Sai, M. V. R., et al. (2019). Retrieval and validation of cloud top temperature from the geostationary satellite INSAT-3D. *Remote Sensing*. **11**(23), 2811.

Loeb, N. G., Várnai, T., and Davies, R. (1997). Effect of cloud inhomogeneities on the solar zenith angle dependence of nadir reflectance. *Journal of Geophysical Research: Atmospheres*. **102**(D8), 9387-9395.

Loeb, N. G., Yang, P., Rose, F. G., et al. (2018). Impact of ice cloud microphysics on satellite cloud retrievals and broadband flux radiative transfer model calculations. *Journal of Climate*. **31,** 1851-1864.

Wolters, E. L. A., Roebeling, R. A., and Feijt, A. J. (2008). Evaluation of cloud-phase retrieval methods for SEVERI on Meteosat-8 using ground-based lidar and cloud radar data. *Journal of Applied Meteorology and Climatology*. **47**, 1723-1738.